Bruton's Tyrosine Kinase Inhibition Attenuates the Cardiac Dysfunction Caused by Cecal Ligation and Puncture in Mice

Caroline E. O'Riordan[1*], Gareth S. D. Purvis[1], Debora Collotta[2], Fausto Chiazza[2], Bianka Wissuwa[3,4], Sura Al Zoubi[1], Lara Stiehler[1,5], Lukas Martin[1,5], Sina M. Coldewey[3,4], Massimo Collino[2], Christoph Thiemermann[1*]

[1]William Harvey Research Institute, Barts and The London School of Medicine and Dentistry, Queen Mary University of London, London, United Kingdom

[2]Department of Drug Science and Technology, University of Turin, Turin, Italy

[3]Department of Anesthesiology and Intensive Care Medicine, Jena University Hospital, Jena, Germany

[4]Septomics Research Center, Jena University Hospital, Jena, Germany

[5]Department of Operative Intensive Care and Intermediate Care, RWTH University Hospital Aachen, Aachen, Germany

*Corresponding authors:

Caroline Elizabeth O'Riordan   Prof. Christoph Thiemermann, MD PhD

c.e.oriordan@qmul.ac.uk   c.thiemermann@qmul.ac.uk

Abstract

Sepsis is one of the most prevalent diseases in the world. The development of cardiac dysfunction in sepsis results in an increase of mortality. It is known that Bruton's tyrosine kinase (BTK) plays a role in toll-like receptor signaling and NLRP3 inflammasome activation, two key components in the pathophysiology of sepsis and sepsis-associated cardiac dysfunction. In this study we investigated whether pharmacological inhibition of BTK (ibrutinib 30 mg/kg and acalabrutinib 3 mg/kg) attenuates sepsis associated cardiac dysfunction in mice. 10-week old male C57BL/6 mice underwent CLP or sham surgery. One hour after surgery mice received either vehicle (5% DMSO + 30% cyclodextrin i.v.), ibrutinib (30 mg/kg i.v.) or acalabrutinib (3 mg/kg i.v.). Mice also received antibiotics and an analgesic at 6 and 18 hours. After 24 hours, cardiac function was assessed by echocardiography *in vivo*. Cardiac tissue underwent western blot analysis to determine the activation of BTK, NLRP3 inflammasome and NF-κB pathway. Serum analysis of 33 cytokines was conducted by a multiplex assay. When compared to sham-operated animals, mice subjected to CLP demonstrated a significant reduction in ejection fraction (EF), fractional shortening (FS) and fractional area change (FAC). The cardiac tissue from CLP mice showed significant increases of BTK, NF-κB, and NLRP3 inflammasome activation. CLP animals resulted in a significant increase of serum cytokines and chemokines (TNF-α, IL-6, IFN-γ, KC, eotaxin-1, eotaxin-2, IL-10, IL-4, CXCL10 and CXCL11). Delayed administration of ibrutinib and acalabrutinib attenuated the decline of EF, FS and FAC caused by CLP and also reduced the activation of BTK, NF-κB and NLRP3 inflammasome. Both ibrutinib and acalabrutinib significantly

40 suppressed the release of cytokines and chemokines. Our study revealed that delayed
41 intravenous administration of ibrutinib or acalabrutinib attenuated the cardiac dysfunction
42 associated with sepsis by inhibiting BTK, reducing NF-κB activation and the activation of the
43 inflammasome. Cytokines associated with sepsis were significantly reduced by both BTK
44 inhibitors. Acalabrutinib is found to be more potent than ibrutinib and could potentially prove
45 to be a novel therapeutic in sepsis. Thus, the FDA-approved BTK inhibitors ibrutinib and
46 acalabrutinib may be repurposed for the use in sepsis.

Introduction

Sepsis is a life-threatening organ dysfunction caused by a dysregulated host response to an infection (1), which affects approximately 30 million people worldwide (2). In the UK, sepsis is the second leading cause of death with 36,000-64,000 patients dying each year (3) costing the NHS £2.5 billion annually (4). The development of cardiac dysfunction affects 40% of septic patients (5) and is associated with an increased mortality rate of 70-90% in comparison to 20% mortality in patients who do not present with cardiac dysfunction (6). However, the mechanisms that underlie this cardiac dysfunction are not well known. Evidence suggests that multiple factors contribute to the pathophysiology of the cardiac dysfunction associated with sepsis. These include the activation of NF-κB and NLRP3 leading to excessive formation of e.g. IL-1 and TNF-α (7,8). There are currently no drugs for the specific treatment of the cardiac dysfunction (or indeed the multiple organ dysfunction) associated with sepsis that specifically target NF-κB and the NLRP3 inflammasome.

Bruton's tyrosine kinase (BTK) plays a role in innate immunity and is a critical component in the development of B cells (9). The FDA has approved the use of the irreversible BTK inhibitors ibrutinib (first generation) in chronic lymphatic leukemia (CLL), mantle cell lymphoma (MCL), Waldenstrom macroglobulinemia (WM) and graft vs. host disease (10) and acalabrutinib (more selective, second generation) in MCL (11). Ibrutinib is also approved by the EMA for the treatment of CLL, MCL and WM (12), whereas acalabrutinib has received an orphan designation for CCL, MCL and lymphoplasmacytic lymphoma (13–15). During sepsis, bacterial LPS stimulates TLR4 and BTK is directly involved in the activation of this signaling pathway. Specifically, BTK binds to the TIR domain of TLR4 and its adaptor molecules (also found in other TLR's) MyD88 and Mal, and results in downstream activation of NF-κB and the generation of proinflammatory cytokines (16). BTK also regulates the assembly and, hence, activation of the NLRP3 inflammasome by binding to the ASC component (17,18). Inhibition of BTK by BTK inhibitors reduces NF-κB activation and the formation of NF-κB-dependent cytokines in murine models of arthritis (19).

Given the importance of TLRs and NLRP3 in the pathophysiology of sepsis, we hypothesized that BTK inhibitors, such as ibrutinib or acalabrutinib, may attenuate the cardiac dysfunction in a murine model of polymicrobial sepsis. Additionally, we set out to investigate the potential effects of BTK inhibition on a) the activation of NF-κB and NLRP3 in the heart, and b) the serum levels of key, pro- and anti-inflammatory cytokines and chemokines.

Methods

Ethical statement

The Animal Welfare Ethics Review Board of Queen Mary University of London approved all experiments in accordance with the Home Office guidance on the operation of Animals (Scientific Procedure Act 1986) published by Her Majesty's Stationary Office, and the Guide for the Care and Use of Laboratory Animals of the National Research Council. Work was conducted under U.K. home office project license number PC5F29685. All *in vivo* experiments are reported in accordance to ARRIVE guidelines (20).

Animals

This study was carried out on 40 ten-week-old male C57BL/6 mice (Charles River Laboratories UK Ltd., Kent, UK) weighing 25-30 g and kept under standard laboratory conditions. Six mice

90 were housed together (in each cage) with access to a chow diet and water *ad libitum*. They
91 were subjected to a 12-hour light and dark cycle with a temperature maintained at 19-23°C.

Drugs

93 Ibrutinib and acalabrutinib were purchased from Selleck Chemicals. Stock solutions were made
94 in DMSO 5% and cyclodextrin 30% (vehicle).

Murine model of polymicrobial sepsis caused by cecum ligation and puncture (CLP)

96 Mice were randomized to undergo either sham operation, CLP + vehicle (5% DMSO + 30%
97 cyclodextrin), CLP + ibrutinib (30 mg/kg) or CLP + acalabrutinib (3 mg/kg). Before surgery,
98 mice were injected with buprenorphine (0.05 mg/kg, i.p.). Mice were initially anesthetized by
99 isoflurane (3 L/min) and oxygen (1 L/min) in an anesthetic chamber and maintained with
100 isoflurane (2 L/min) and oxygen (1 L/min) via a face mask. Temperature was monitored via a
101 rectal probe and kept at 37°C by a homeothermic mat. Veet® hair removal cream was used to
102 remove the fur from the abdomen of the mouse and skin was then cleaned with 70% ethanol.
103 The abdomen was opened with a 1.5 cm midline incision to expose the cecum. The cecum was
104 fully ligated below the ileocecal valve, and a G-18 needle was used to puncture two holes in
105 the top and bottom of the cecum. A small amount of feces was then squeezed out. The cecum
106 was returned to the abdomen in its anatomical position and 5 ml/kg of saline was administered
107 into the abdomen before its closure. Saline (10 ml/kg s.c.) was administered directly after
108 surgery. One hour after CLP, vehicle (5% DMSO + 30% cyclodextrin), ibrutinib (30 mg/kg),
109 or acalabrutinib (3 mg/kg) was administered intravenously. At 6 and 18 h after surgery,
110 antibiotics (imipenem/cilastatin; 20 mg/kg dissolved in saline s.c.) and an analgesic
111 (buprenorphine; 0.05 mg/kg i.p.) were administered. After 24 h, cardiac function was assessed
112 by echocardiography *in vivo*. Mice that underwent sham surgery were not subjected to ligation
113 or perforation of the cecum but were otherwise treated the same way, 1 h after surgery sham
114 animals were treated with vehicle (5% DMSO + 30% cyclodextrin).

Renal dysfunction analysis

116 Renal dysfunction was analysed in all mice. The mice were anaesthetised with isoflurane (3
117 L/min) and oxygen (1 L/min) before being sacrificed. Cardiac puncture was performed with a
118 G25 needle and non-heparinized syringes to obtain approximately 0.7 ml of blood. The blood
119 was immediately decanted into 1.3 ml serum gel tubes (Sarstedt, Nürnbrecht, Germany). The
120 heart and lungs were then removed. The blood samples were centrifuged for 3 min at 9000
121 RPM to separate the serum, where 100 µL of serum was pipetted into an aliquot and snap
122 frozen in liquid nitrogen and stored at -80°C for further analysis. The serum was then sent to
123 an independent veterinary testing laboratory (MRC Harwell Institute, Oxford, UK) to blindly
124 quantify serum urea and creatinine known markers of renal dysfunction.

Echocardiography

126 At 24 h after CLP, cardiac function was assessed with a Vevo 3100 imaging system
127 (VisualSonics, Toronto, Ontario, Canada). Mice were fully sedated in an anesthetic chamber
128 with isoflurane (3 L/min) and oxygen (1 L/min) and were then transferred to the
129 thermoregulatory platform in the supine position, where their paws were taped on to the EKG
130 leads. Anesthetic was maintained throughout the entire procedure via a nosecone with
131 isoflurane (0.5-2.0 L/min) and oxygen (1 L/min). The fur on the chest was removed by Veet®
132 hair removal cream and pre-warmed echo gel was placed onto the shaven chest. The heart was

133 then imaged with the MX550D imaging probe. To measure the left ventricle in B-mode the
134 probe was placed along the long axis of the left ventricle, and directed towards the right of the
135 mouse, here we measured percentage fractional area change (FAC %). The probe was then
136 rotated 90° to visualize the short axis in the M-mode where the following parameters were
137 measured: the percentage ejection fraction (EF %) and fractional shortening (FS %).

Western blot analysis

139 Immunoblot analyses of cardiac tissue samples were carried out using a semi-quantitative
140 western blotting analysis. The antibody used were: 1:1000 rabbit anti-Ser$^{176/180}$-IKKα/β,
141 1:1000 rabbit anti-total IKKα/β, 1:1000 mouse anti-Ser$^{32/36}$-IκBα, 1:1000 mouse anti-total
142 IκBα , 1:1000 rabbit anti-NF-κB, 1:1000 rabbit anti-total BTK, 1:1000 rabbit anti-Tyr^{1217}
143 PLCγ, 1:1000 rabbit anti-total PLCγ (from Cell Signaling), 1:1000 rabbit anti-Tyr^{223}-BTK,
144 1:5000 rabbit anti NLRP3 inflammasome (from Abcam), 1:1000 mouse anti-caspase 1 (p20)
145 (from Adipogen). The apex of the heart was taken and homogenized in 1:10 of homogenization
146 buffer at 4°C. Nuclear and cytosolic proteins were then extracted as previously described (21)
147 and concentrations were quantified by bicinchoninic acid (BCA) protein assay (Thermo Fisher
148 Scientific Rockford, IL). Proteins were separated by 8% sodium dodecyl sulphate (SDS)-
149 PAGE and transferred to polyvinyldenedifluoride membranes. Membranes were blocked in
150 10% milk solution with TBS-Tween and then incubated with the primary antibody overnight
151 at 4°C. The next day the secondary antibody was added for 30 min at room temperature and
152 visualized using the ECL detection system. Tubulin and and histone 3 were used as loading
153 control. The immunoreactive bands were analyzed by the Bio-Rad Image Lab Software^{TM} 6.0.1
154 and results were normalized to the sham bands.

Multiplex flow immunoassay

156 The principle of multiplex flow immunoassay technology has been reviewed previously
157 (22,23). Cytokines, chemokines and a growth factor were determined in serum by Bio-Plex Pro
158 Mouse Chemokine 33-plex panel assay (Bio-Rad, Kabelsketal, Germany). The cytokines IL-
159 1ß, -2, -4, -6, -10, -16, CCL1, -2, -3, -4, -5, -7, -11, -12, -17, -19, -20, -22, -24, -25, -27, IFN-
160 γ, TNF-α and the chemokines CX3CL1, CXCL1, -2, -5, -10, -11, -12, -13, -16 and the growth
161 factor GM-CSF were measured according to the manufacturer's instructions. The assays were
162 performed in one batch, with samples randomly distributed. The lower detection limit was 3.2
163 pg/ml for all the analytes. Data were collected and analyzed using a Bio-Plex® 200 instrument
164 equipped with Bio-Plex Manager software (Bio-Rad).

Statistical analysis

166 All data in text and figures are expressed as mean ± standard error mean (SEM) of n
167 observations. Measurements obtained from the intervention, control and sham were analyzed
168 by one-way ANOVA followed by a Bonferroni's *post hoc* test on GraphPad Prism 6.0
169 (GraphPad Software, Inc., La Jolla, CA, USA). Correlations coefficients were determined by
170 Pearson's correlation with P values based on two-tailed tests. Differences were considered to
171 be statistically significant when $P < 0.05$.

Results

Ibrutinib or acalabrutinib attenuate the cardiac dysfunction caused by CLP-sepsis

When compared to sham-operated animals, mice subjected to CLP for 24 h (Figure 1A) demonstrated a significant reduction in EF, FS and FAC ($P < 0.0001$; Figure 1B-E) indicating the development of systolic cardiac dysfunction. The observed reduction in EF also negatively correlated with the rise of the chemokines CXCL10 and CXCL11, both of which are well known biomarkers of left ventricular dysfunction (Figure 1F-I). When compared to CLP mice treated with vehicle (control), the administration of ibrutinib (30 mg/kg) or acalabrutinib (3 mg/kg) at 1 h after CLP significantly attenuated the decline in EF, FS and FAC caused by CLP ($P < 0.01$; Figure 1 B-E). The rise in the serum levels of the chemokines CXCL10 and CXCL11 caused by CLP were also significantly reduced by either ibrutinib or acalabrutinib ($P < 0.05$, Figure 1F-I). No significant differences were observed in any of the cardiac parameters or cytokines measured in CLP animals treated with either ibrutinib or acalabrutinib ($P > 0.05$; Figure 1 B-I). To gain a better insight into the mechanism by which the two BTK-inhibitors reduce the cardiac dysfunction associated with sepsis, we investigated the effects of ibrutinib and acalabrutinib on a) BTK-activation and signaling, b) NF-κB activation and c) NLRP3 inflammasome assembly and activation (see below).

Ibrutinib or acalabrutinib attenuate the renal dysfunction caused by CLP-sepsis

Urea and creatinine were measured to study the effect of CLP (in the absence and presence of BTK inhibitors) on kidney function. When compared to sham, mice subjected to CLP and treated with vehicle had a significant increase of urea and creatinine, indicating kidney dysfunction (Figure 2, $P < 0.0001$). Administration of ibrutinib (30 mg/kg) or acalabrutinib (3 mg/kg) to CLP mice significantly attenuated the rise in urea and creatinine when compared to CLP mice treated with vehicle (Figure 2, $P < 0.01$), without any significant difference between the two treatment.

Cardiac BTK is activated in CLP mice and reduced by ibrutinib or acalabrutinib

Using Western blot analysis, we investigated whether CLP-sepsis leads to an activation of BTK in the heart. The activation of BTK and the subsequent activation of BTK-signaling involves a) phosphorylation of BTK at Tyr^{223} and b) the phosphorylation of PLCγ at Tyr^{1217} by phosphorylated (activated) BTK as the first step in the BTK-signaling cascade. When compared to sham operated mice, CLP mice treated with vehicle demonstrated significant increases in the phosphorylation of cardiac BTK at Tyr^{223} and the phosphorylation of PLCγ at Tyr^{1217}, indicating that BTK is activated in septic hearts ($P < 0.0001$, Figure 3A). Administration of ibrutinib (30 mg/kg) or acalabrutinib (3 mg/kg) in CLP mice resulted in a significant decrease in the phosphorylation of cardiac BTK at Tyr^{223} and the phosphorylation of PLCγ at Tyr^{1217} when compared to CLP mice treated with vehicle ($P < 0.0001$, Figure 3B) demonstrating that the doses of the two BTK inhibitors used in our study caused a significant inhibition of BTK-signaling in the heart. No significant differences were observed in the degree of phosphorylation of cardiac BTK at Tyr^{223} and the phosphorylation of PLCγ at Tyr^{1217} in CLP-animals treated with either ibrutinib or acalabrutinib ($P > 0.05$, Figure 3A&B).

Cardiac NF-κB activation in CLP mice is reduced by ibrutinib or acalabrutinib

To understand the signaling mechanism associated with the observed cardiac dysfunction, we investigated the effect of BTK inhibition on the activation of key signaling pathways of inflammation including pathways leading to the activation of NF-κB. When compared to sham operated mice, CLP mice treated with vehicle had significant increases in the phosphorylation of IKKα/β at $Ser^{176/180}$, the phosphorylation of IκBα at $Ser^{32/36}$ and the translocation of p65 to the nucleus ($P < 0.001$, Figure 4A-C). When compared with CLP mice treated with vehicle, treatment of CLP mice with ibrutinib (30 mg/kg) or acalabrutinib (3 mg/kg) significantly attenuated the increases in cardiac phosphorylation of IKKα/β at $Ser^{176/180}$ and IκBα at $Ser^{32/36}$ and the nuclear translocation of p65 ($P < 0.0001$, Figure 4A-C). No significant differences were observed in the degree of phosphorylation of IKKα/β at $Ser^{176/180}$, the phosphorylation of IκBα at $Ser^{32/36}$ and the translocation of p65 to the nucleus in CLP animals treated with either ibrutinib or acalabrutinib ($P > 0.05$, Figure 4A-C).

Cardiac NLRP3 activation in CLP mice is reduced by ibrutinib or acalabrutinib

We next assessed the potential involvement of NLRP3 in the cardiac dysfunction of CLP mice. When compared to sham operated mice, CLP-sepsis (vehicle-treatment) resulted in the increased expression of the NLRP3 inflammasome and cleavage of pro-caspase-1 to caspase-1 in the heart and a rise in serum IL-1β ($P < 0.0001$, Figure 5A-C). When compared to CLP mice treated with vehicle, treatment of CLP mice with ibrutinib or acalabrutinib significantly inhibited the expression of NLRP3, cleavage of pro-caspase-1 to caspase-1 and the rise in IL-1β ($P < 0.01$, Figure 5A-C), without any significant difference between the two drug treatments.

Relationship between BTK activation and cardiac dysfunction in CLP-sepsis

To address the question whether the degree of activation of BTK correlates with alterations in cardiac function, we correlated the degree of phosphorylation of BTK at Tyr^{223} (Figure 6A) and the phosphorylation of PLCγ at Tyr^{1217} (Figure 6B) with EF. We found a highly significant negative correlation between the degree of BTK and PLCγ activation and the decline in EF, strongly suggesting that BTK activation drives or precedes the cardiac dysfunction associated with sepsis. To address the question whether the degree of activation of BTK also correlates with alterations in the activation of NF-κB, we correlated the degree of phosphorylation of BTK at Tyr^{223} with the translocation of p65 (Figure 6C) and the phosphorylation of IKKα/β at $Ser^{176/180}$ (Figure 6D). We found a highly significant positive correlation between the degree of BTK activation and the activation of NF-κB when measured as either the translocation of p65 (Figure 6C) and the phosphorylation of IKKα/β at $Ser^{176/180}$ (Figure 6D). To address the question whether the degree of activation of BTK also correlates with alterations in the assembly and activation of the inflammasome, we correlated the degree of phosphorylation of BTK at Tyr^{223} with either NLRP3 assembly (Figure 6E) or the activation of caspase-1 (Figure 6F). We found a highly significant positive correlation between the degree of BTK activation and the NLRP3 (Figure 6E) increased expression and the activation of caspase-1 (Figure 6F).

Systemic inflammation in CLP mice is reduced by ibrutinib or acalabrutinib

We also studied the effect of CLP (in the absence and presence of BTK inhibitors) on the systemic synthesis of pro-inflammatory cytokines, anti-inflammatory cytokines and pro-inflammatory chemokines. When compared to sham operated mice, CLP (vehicle) resulted in a significant rise in the serum levels of a) the pro-inflammatory cytokines TNF-α, IFN-γ, IL-6; b) the anti-inflammatory cytokines IL-4 and IL-10, and c) the pro-inflammatory chemokines

257   KC/CXCL1, eotaxin-1/CCL11, eotaxin-2/CCL24 ($P < 0.05$, Figure 7A-H). The sepsis-induced
258   increase in these cytokines and chemokines was significantly attenuated by both BTK
259   inhibitors, the only exception being IL-6, which was not significantly reduced by ibrutinib but
260   a trend in reduction was observed. No significant differences were observed in the levels of
261   cytokines or chemokines in CLP animals treated with either ibrutinib or acalabrutinib ($P >$
262   0.05, Figure 7A-H).

263   The data of all other cytokines/chemokines/growth factors that we measured in all groups are
264   provided in Supplemental Figure S1.

Discussion

We show here, for the first time, that administration of two structurally different BTK inhibitors (ibrutinib and acalabrutinib) both ameliorate the cardiac dysfunction (measured as decline in EF, FS or FAC by echocardiography) caused by CLP-sepsis. The observed decline in EF also was associated with a significant increase in the serum levels of two, well-known biomarkers of left ventricular dysfunction, namely CXCL10 and CXCL11 (24–26). Most notably, ibrutinib or acalabrutinib also attenuated the rises in CXCL10 and CXCL11 caused by CLP-sepsis. In addition, ibrutinib or acalabrutinib also reduced the renal dysfunction (measured as increase in serum urea or creatinine) caused by CLP-sepsis. Thus, both BTK inhibitors reduced the cardiac and renal dysfunction caused by sepsis.

What, then, is the mechanism by which ibrutinib or acalabrutinib reduce the cardiac (renal) dysfunction caused by sepsis? Ibrutinib is a potent BTK inhibitor, but not very specific (as it also inhibits a multitude of other kinases), which is approved by the FDA and the EMA for the use in CLL, MCL and WM. Acalabrutinib is a potent, but highly specific BTK inhibitor: At a (relatively high) concentration of 1 μM, acalabrutinib strongly inhibited only the following 5 kinases: BTK, Bmx, ErbB4, RIPK2 and TEC, while the same concentration of ibrutinib inhibited 35 kinases. It should be noted that the doses of acalabrutinib and ibrutinib that we used in our study in the mouse resulted in a similar, approximately 70%, inhibition of BTK activity in septic hearts. We, therefore, propose that inhibition of BTK activity explains the observed beneficial effects of ibrutinib or acalabrutinib in sepsis. The activation of BTK and the subsequent activation of BTK signaling involves a) phosphorylation of BTK at Tyr^{223} and b) the phosphorylation of PLCγ at Tyr^{1217} by phosphorylated (activated) BTK as the first step in the BTK signaling cascade (27). We report here that sepsis results in significant increases in the phosphorylation of cardiac BTK at Tyr^{223} and the phosphorylation of PLCγ at Tyr^{1217}, indicating that BTK is activated in septic hearts. Most notably, the activation of BTK negatively correlated with EF indicating that activation of BTK is associated with the cardiac dysfunction in sepsis. Indeed, inhibition of BTK activity with ibrutinib or acalabrutinib in the heart of septic animals reduces the cardiac dysfunction in sepsis suggesting that activation of BTK plays a pivotal role in the pathophysiology of the cardiac dysfunction in sepsis.

What are the mechanisms by which the activation of BTK (in the heart) leads to cardiac dysfunction in sepsis? There is good evidence that a) the activation of BTK precedes the activation of NF-κB (16), and b) the activation of NF-κB plays an important role in the cardiac dysfunction in sepsis (28,29). Specifically, inhibition of the activity of NF-κB attenuates the cardiac dysfunction in sepsis (30,31). We report here, for the first time, that a) activation of BTK is associated activation of NF-κB in septic hearts, and b) inhibition of BTK activity with ibrutinib or acalabrutinib reduces both the activation of NF-κB in septic hearts and the cardiac dysfunction caused by sepsis. Thus, we propose that inhibition of the activation of NF-κB contributes to the observed beneficial effects of the BTK inhibitors ibrutinib and acalabrutinib in sepsis. When challenging BTK KO-mice with LPS, Gabhann and colleagues observed reduced i) activation of NF-κB p65, ii) Akt phosphorylation and iii) M1 polarisation of macrophages (32).

Activation of NF-κB drives the formation of a number of pro- and anti-inflammatory cytokines and chemokines. We report here that CLP-sepsis leads to a significant increase in the serum levels of the pro-inflammatory cytokines TNF-α, IL-6, IFN-γ, anti-inflammatory cytokines IL-10, IL-4 and the chemokines KC/CXCL1, eotaxin-1/CCL11, eotaxin-2/CCL24, all of which importantly contribute to the local and systemic inflammation and organ injury associated with

311 sepsis (33). Most notably, we see the powerful pro-inflammatory cytokine TNF-α to be
312 ameliorated by both BTK inhibitors. TNF-α has been implicated in murine models of sepsis
313 and in humans with sepsis. TNF-α acts in an autocrine and paracrine manner leading to
314 macrophage production and activation, resulting in the release of other proinflammatory
315 cytokines such as IL-6 and IL-8 (34,35).

316 Similarly, there is also good evidence that activation of BTK plays a crucial role in the
317 assembly and activation of the NLRP3 inflammasome (17,36). The activation of the NLRP3
318 inflammasome has been suggested to play a role in the cardiac dysfunction (37) and the
319 pathophysiology of sepsis (38). Others have reported that inhibition of the assembly and
320 activation of NLRP3 inflammasome protects against microbial sepsis (38). We report here for
321 the first time that a) activation of BTK is associated with the activation of the NLRP3
322 inflammasome in septic hearts, and b) inhibition of BTK activity with ibrutinib and
323 acalabrutinib reduces both the assembly and subsequent activation of the NLRP3
324 inflammasome in septic hearts (and the cardiac dysfunction caused by sepsis). Thus, we
325 propose that inhibition of the activation of the NLRP3 inflammasome may also contribute to
326 the observed beneficial effects of the BTK inhibitors ibrutinib and acalabrutinib in sepsis.

327 Activation of the NLRP3 inflammasome drives the formation of IL-1β and IL-18, both of
328 which play an important role in the systemic inflammation and/or organ dysfunction in sepsis
329 (39). Specifically, inhibition of caspase-1 results in an inhibition of IL-18 and IL-1β secretion,
330 which, in turn, attenuated the cardiac dysfunction caused by myocardial ischemia (40). The
331 role of the inflammasome in the pathophysiology of sepsis, however, is still controversial: For
332 example, survival was similar in wild-type and caspase-1/11 knockout mice with sepsis, while
333 the neutralization of IL-1 and IL-18 reduced mortality in endotoxemia (39). Here we show that
334 BTK inhibition results in reduced serum levels of IL-1β, and this was associated with an
335 improvement of cardiac function.

336 The evaluation of the efficacy of the BTK inhibitors used in our study depends on the
337 assumption that the development of organ dysfunction (and specifically cardiac and renal
338 dysfunction) correlates with outcome. There is good evidence that the occurrence of cardiac
339 and/or renal dysfunction correlates positively with an increase in mortality in patients with
340 sepsis (6). We have, however, not investigated the effects of BTK inhibition on survival in
341 animals with sepsis due to ethical reasons. It would be useful to confirm whether inhibition of
342 BTK activity does, indeed, improve survival in longer models of sepsis (rather than the very
343 acute model employed here).

344 In addition to inhibiting BTK, ibrutinib and acalabrutinib also strongly inhibit four other
345 kinases. To ensure that inhibition of BTK, indeed, accounts for the inhibition of NF-κB and
346 the inflammasome and ultimately the observed beneficial effects in sepsis, it would be useful
347 to repeat our study in BTK knockout mice. Interestingly, of the kinases which are strongly
348 inhibited by ibrutinib and acalabrutinib, expression of ErbB4 (rather than its activation) may
349 play a role in the cardiac dysfunction and cognitive impairment associated with sepsis (41). In
350 contrast, RIP2 kinase is unlikely to play a significant role in sepsis, as the CLP-induced septic
351 peritonitis was similar in RIP2 knockout mice and their wild-type litter mates (42).

352 **Conclusions**

353 There are currently no specific treatments, which reduce the cardiac dysfunction or, indeed,
354 mortality in sepsis. Our data shows for the first time that two commercially available BTK

inhibitors, ibrutinib or acalabrutinib, attenuate the CLP-induced cardiac dysfunction through inhibition of the activation of BTK/NF-κB and/or the NLRP3 inflammasome, which in turn reduces the formation of a number of chemokines and cytokines including TNF-α. Notably, no significant qualitative or quantitative differences were found with two, chemically distinct BTK-inhibitors suggesting that the observed beneficial effects of both compounds in experimental sepsis are likely to be a drug class related effect. Thus, BTK inhibitors are FDA-approved drugs that maybe repurposed for the use in sepsis, but also for other diseases associated with either local or systemic inflammation.

Conflict of interests: The authors declare that they do not have any conflicts of interests.

Author contributions: Conceived and designed the experiment: CEO, GSDP, SMC, MC, CT. Performed the experiments: CEO, GSDP, DC, FC, BW, SZ, LS. Analyzed the data: CEO, MC SMC, BW, LM, CT. Contributed to the writing of the manuscript: CEO, CT. Contributed to the revision prior to submission MC, FC, SMC, BW, LM, SZ.
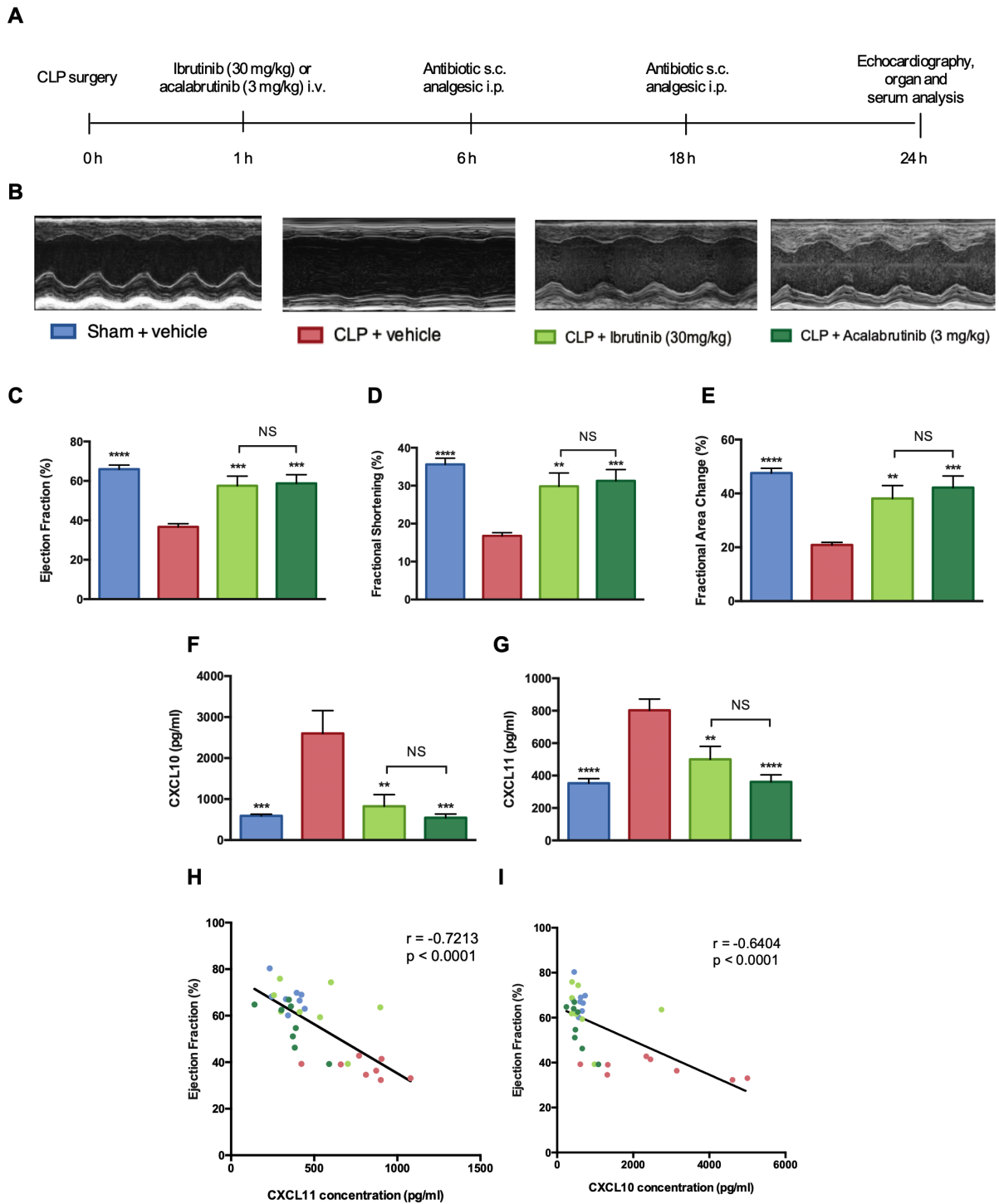
References:

1. Singer M, Deutschman CS, Seymour CW, Shankar-Hari M, Annane D, Bauer M, Bellomo R, Bernard GR, Chiche J-D, Coopersmith CM, et al. The Third International Consensus Definitions for Sepsis and Septic Shock (Sepsis-3). *JAMA* (2016) **315**:801–10. doi:10.1001/jama.2016.0287

2. Fleischmann C, Scherag A, Adhikari NKJ, Hartog CS, Tsaganos T, Schlattmann P, Angus DC, Reinhart K. Assessment of Global Incidence and Mortality of Hospital-treated Sepsis. Current Estimates and Limitations. *Am J Respir Crit Care Med* (2016) **193**:259–272. doi:10.1164/rccm.201504-0781OC

3. Daniels R. Surviving the first hours in sepsis: getting the basics right (an intensivist's perspective). *J Antimicrob Chemother* (2011) **66**:ii11–ii23. doi:10.1093/jac/dkq515

4. Richards M. Sepsis management as an NHS clinical priority. UK sepsis group. (2014) Available at: http://www.england.nhs.uk/wp-content/uploads/2013/12/sepsis-brief.pdf [Accessed March 1, 2019]

5. Hunter JD, Doddi M. Sepsis and the heart. *Br J Anaesth* (2010) **104**:3–11. doi:10.1093/BJA/AEP339

6. Parrillo JE, Parker MM, Natanson C, Suffredini AF, Danner RL, Cunnion RE, Ognibene FP. Septic Shock in Humans. *Ann Intern Med* (1990) **113**:227.

396   doi:10.7326/0003-4819-113-3-227

397   7.   Kumar A, Thota V, Dee L, Olson J, Uretz E, Parrillo JE. Tumor necrosis factor alpha
398   and interleukin 1beta are responsible for in vitro myocardial cell depression induced
399   by human septic shock serum. *J Exp Med* (1996) **183**:949–58. Available at:
400   http://www.ncbi.nlm.nih.gov/pubmed/8642298 [Accessed March 1, 2019]

401   8.   Martin L, Derwall M, Al Zoubi S, Zechendorf E, Reuter DA, Thiemermann C,
402   Schuerholz T. The Septic Heart: Current Understanding of Molecular Mechanisms and
403   Clinical Implications. *Chest* (2019) **155**:427–437. doi:10.1016/J.CHEST.2018.08.1037

404   9.   Tsukada S, Saffran DC, Rawlings DJ, Parolini O, Allen RC, Klisak I, Sparkes RS,
405   Kubagawa H, Mohandas T, Quan S. Deficient expression of a B cell cytoplasmic
406   tyrosine kinase in human X-linked agammaglobulinemia. *Cell* (1993) **72**:279–90.
407   Available at: http://www.ncbi.nlm.nih.gov/pubmed/8425221 [Accessed February 12,
408   2019]

409   10.   Sanford DS, Wierda WG, Burger JA, Keating MJ, O'Brien SM. Three Newly
410   Approved Drugs for Chronic Lymphocytic Leukemia: Incorporating Ibrutinib,
411   Idelalisib, and Obinutuzumab into Clinical Practice. *Clin Lymphoma Myeloma Leuk*
412   (2015) **15**:385–391. doi:10.1016/j.clml.2015.02.019

413   11.   Markham A, Dhillon S. Acalabrutinib: First Global Approval. *Drugs* (2018) **78**:139–
414   145. doi:10.1007/s40265-017-0852-8

415   12.   European Medicines Agency. Imbruvica. (2019) Available at:
416   https://www.ema.europa.eu/en/medicines/human/EPAR/imbruvica

417   13.   European Medicines Agency. Orphan designation: Acalabrutinib for: Treatment of
418   chronic lymphocytic leukaemia / small lymphocytic lymphoma. (2016) Available at:
419   https://www.ema.europa.eu/en/medicines/human/orphan-designations/eu3161626

420   14.   European Medicines Agency. Orphan designation: Acalabrutinib for: Treatment of
421   lymphoplasmacytic lymphoma. (2016) Available at:
422   https://www.ema.europa.eu/en/medicines/human/orphan-designations/eu3161626

423   15.   European Medicines Agency. Orphan designation: Acalabrutinib for: Treatment of
424   mantle cell lymphoma. (2016) Available at:
425   https://www.ema.europa.eu/en/medicines/human/orphan-designations/eu3161625

426   16.   Jefferies CA, Doyle S, Brunner C, Dunne A, Brint E, Wietek C, Walch E, Wirth T,
427   O'Neill LAJ. Bruton's tyrosine kinase is a Toll/interleukin-1 receptor domain-binding
428   protein that participates in nuclear factor kappaB activation by Toll-like receptor 4. *J
429   Biol Chem* (2003) **278**:26258–64. doi:10.1074/jbc.M301484200

430   17.   Liu X, Pichulik T, Wolz O-O, Dang T-M, Stutz A, Dillen C, Delmiro Garcia M, Kraus
431   H, Dickhöfer S, Daiber E, et al. Human NACHT, LRR, and PYD domain–containing
432   protein 3 (NLRP3) inflammasome activity is regulated by and potentially targetable
433   through Bruton tyrosine kinase. *J Allergy Clin Immunol* (2017) **140**:1054-1067.e10.
434   doi:10.1016/J.JACI.2017.01.017

435   18.   Ito M, Shichita T, Okada M, Komine R, Noguchi Y, Yoshimura A, Morita R. Bruton's

12

436 tyrosine kinase is essential for NLRP3 inflammasome activation and contributes to
437 ischaemic brain injury. *Nat Commun* (2015) **6**:7360. doi:10.1038/ncomms8360

438 19. Wu H, Huang Q, Qi Z, Chen Y, Wang A, Chen C, Liang Q, Wang J, Chen W, Dong J,
439   et al. Irreversible inhibition of BTK kinase by a novel highly selective inhibitor
440   CHMFL-BTK-11 suppresses inflammatory response in rheumatoid arthritis model. *Sci*
441   *Rep* (2017) **7**:466. doi:10.1038/s41598-017-00482-4

442 20. Kilkenny C, Browne WJ, Cuthill IC, Emerson M, Altman DG. Improving Bioscience
443   Research Reporting: The ARRIVE Guidelines for Reporting Animal Research. *PLoS*
444   *Biol* (2010) **8**:e1000412. doi:10.1371/journal.pbio.1000412

445 21. Collino M, Pini A, Mugelli N, Mastroianni R, Bani D, Fantozzi R, Papucci L, Fazi M,
446   Masini E. Beneficial effect of prolonged heme oxygenase 1 activation in a rat model of
447   chronic heart failure. *Dis Model Mech* (2013) **6**:1012–20. doi:10.1242/dmm.011528

448 22. Morgan E, Varro R, Sepulveda H, Ember JA, Apgar J, Wilson J, Lowe L, Chen R,
449   Shivraj L, Agadir A, et al. Cytometric bead array: a multiplexed assay platform with
450   applications in various areas of biology. *Clin Immunol* (2004) **110**:252–266.
451   doi:10.1016/j.clim.2003.11.017

452 23. Varro R, Chen R, Sepulveda H, Apgar J. "Bead-Based Multianalyte Flow
453   Immunoassays," in *Methods in molecular biology (Clifton, N.J.)*, 125–152.
454   doi:10.1007/978-1-59745-323-3_9

455 24. Altara R, Mallat Z, Booz GW, Zouein FA. The CXCL10/CXCR3 Axis and Cardiac
456   Inflammation: Implications for Immunotherapy to Treat Infectious and Noninfectious
457   Diseases of the Heart. *J Immunol Res* (2016) **2016**:4396368.
458   doi:10.1155/2016/4396368

459 25. Altara R, Manca M, Hessel MH, Gu Y, van Vark LC, Akkerhuis KM, Staessen JA,
460   Struijker-Boudier HAJ, Booz GW, Blankesteijn WM. CXCL10 Is a Circulating
461   Inflammatory Marker in Patients with Advanced Heart Failure: a Pilot Study. *J*
462   *Cardiovasc Transl Res* (2016) **9**:302–314. doi:10.1007/s12265-016-9703-3

463 26. Altara R, Gu Y-M, Struijker-Boudier HAJ, Thijs L, Staessen JA, Blankesteijn WM.
464   Left Ventricular Dysfunction and CXCR3 Ligands in Hypertension: From Animal
465   Experiments to a Population-Based Pilot Study. *PLoS One* (2015) **10**:e0141394.
466   doi:10.1371/journal.pone.0141394

467 27. Kurosaki T, Maeda A, Ishiai M, Hashimoto A, Inabe K, Takata M. Regulation of the
468   phospholipase C-gamma2 pathway in B cells. *Immunol Rev* (2000) **176**:19–29.
469   Available at: http://www.ncbi.nlm.nih.gov/pubmed/11043765 [Accessed March 19,
470   2019]

471 28. Pritts TA, Moon MR, Wang Q, Hungness ES, Salzman AL, Fischer JE, Hasselgren
472   PO. Activation of NF-kappaB varies in different regions of the gastrointestinal tract
473   during endotoxemia. *Shock* (2000) **14**:118–22. Available at:
474   http://www.ncbi.nlm.nih.gov/pubmed/10947153 [Accessed February 25, 2019]

475 29. Liu SF, Ye X, Malik AB. Pyrrolidine dithiocarbamate prevents I-kappaB degradation
476   and reduces microvascular injury induced by lipopolysaccharide in multiple organs.

477   *Mol Pharmacol* (1999) **55**:658–67. Available at:
478   http://www.ncbi.nlm.nih.gov/pubmed/10101023 [Accessed February 25, 2019]

479 30. Al Zoubi S, Chen J, Murphy C, Martin L, Chiazza F, Collotta D, Yaqoob MM, Collino
480   M, Thiemermann C. Linagliptin Attenuates the Cardiac Dysfunction Associated With
481   Experimental Sepsis in Mice With Pre-existing Type 2 Diabetes by Inhibiting NF-κB.
482   *Front Immunol* (2018) **9**:2996. doi:10.3389/fimmu.2018.02996

483 31. Chen J, Kieswich JE, Chiazza F, Moyes AJ, Gobbetti T, Purvis GSD, Salvatori DCF,
484   Patel NSA, Perretti M, Hobbs AJ, et al. IκB Kinase Inhibitor Attenuates Sepsis-
485   Induced Cardiac Dysfunction in CKD. *J Am Soc Nephrol* (2017) **28**:94–105.
486   doi:10.1681/ASN.2015060670

487 32. Ní Gabhann J, Hams E, Smith S, Wynne C, Byrne JC, Brennan K, Spence S,
488   Kissenpfennig A, Johnston JA, Fallon PG, et al. Btk regulates macrophage polarization
489   in response to lipopolysaccharide. *PLoS One* (2014) **9**:e85834.
490   doi:10.1371/journal.pone.0085834

491 33. Chaudhry H, Zhou J, Zhong Y, Ali MM, McGuire F, Nagarkatti PS, Nagarkatti M.
492   Role of cytokines as a double-edged sword in sepsis. *In Vivo* (2013) **27**:669–84.
493   Available at: http://www.ncbi.nlm.nih.gov/pubmed/24292568 [Accessed March 26,
494   2019]

495 34. Fong Y, Tracey KJ, Moldawer LL, Hesse DG, Manogue KB, Kenney JS, Lee AT, Kuo
496   GC, Allison AC, Lowry SF. Antibodies to cachectin/tumor necrosis factor reduce
497   interleukin 1 beta and interleukin 6 appearance during lethal bacteremia. *J Exp Med*
498   (1989) **170**:1627–33. doi:10.1084/JEM.170.5.1627

499 35. Cohen J. The immunopathogenesis of sepsis. *Nature* (2002) **420**:885–891.
500   doi:10.1038/nature01326

501 36. Ito M, Shichita T, Okada M, Komine R, Noguchi Y, Yoshimura A, Morita R. Bruton's
502   tyrosine kinase is essential for NLRP3 inflammasome activation and contributes to
503   ischaemic brain injury. *Nat Commun* (2015) **6**:7360. doi:10.1038/ncomms8360

504 37. Zhang W, Xu X, Kao R, Mele T, Kvietys P, Martin CM, Rui T. Cardiac Fibroblasts
505   Contribute to Myocardial Dysfunction in Mice with Sepsis: The Role of NLRP3
506   Inflammasome Activation. *PLoS One* (2014) **9**:e107639.
507   doi:10.1371/journal.pone.0107639

508 38. Lee S, Nakahira K, Dalli J, Siempos II, Norris PC, Colas RA, Moon J-S, Shinohara M,
509   Hisata S, Howrylak JA, et al. NLRP3 Inflammasome Deficiency Protects against
510   Microbial Sepsis via Increased Lipoxin B 4 Synthesis. *Am J Respir Crit Care Med*
511   (2017) **196**:713–726. doi:10.1164/rccm.201604-0892OC

512 39. Berghe T Vanden, Demon D, Bogaert P, Vandendriessche B, Goethals A, Depuydt B,
513   Vuylsteke M, Roelandt R, Van Wonterghem E, Vandenbroecke J, et al. Simultaneous
514   Targeting of IL-1 and IL-18 Is Required for Protection against Inflammatory and
515   Septic Shock. *Am J Respir Crit Care Med* (2014) **189**:282–291.
516   doi:10.1164/rccm.201308-1535OC

517 40. Pomerantz BJ, Reznikov LL, Harken AH, Dinarello CA. Inhibition of caspase 1

518   reduces human myocardial ischemic dysfunction via inhibition of IL-18 and IL-1beta.
519   *Proc Natl Acad Sci U S A* (2001) **98**:2871–6. doi:10.1073/pnas.041611398

520   41.   An R, Feng J, Xi C, Xu J, Sun L. miR-146a Attenuates Sepsis-Induced Myocardial
521   Dysfunction by Suppressing IRAK1 and TRAF6 via Targeting ErbB4 Expression.
522   *Oxid Med Cell Longev* (2018) **2018**:1–9. doi:10.1155/2018/7163057

523   42.   Sônego F, Castanheira FVS, Czaikoski PG, Kanashiro A, Souto FO, França RO,
524   Nascimento DC, Freitas A, Spiller F, Cunha LD, et al. MyD88-, but not Nod1- and/or
525   Nod2-deficient mice, show increased susceptibility to polymicrobial sepsis due to
526   impaired local inflammatory response. *PLoS One* (2014) **9**:e103734.
527   doi:10.1371/journal.pone.0103734

528

Legends to figures

A

CLP surgery | Ibrutinib (30 mg/kg) or acalabrutinib (3 mg/kg) i.v. | Antibiotic s.c. analgesic i.p. | Antibiotic s.c. analgesic i.p. | Echocardiography, organ and serum analysis

0 h   1 h   6 h   18 h   24 h

B

Sham + vehicle   CLP + vehicle   CLP + Ibrutinib (30mg/kg)   CLP + Acalabrutinib (3 mg/kg)

C

D

E

F


G

H

r = -0.7213
p < 0.0001

I

r = -0.6404
p < 0.0001

Figure 1: Ibrutinib or acalabrutinib attenuate the cardiac dysfunction caused by CLP-sepsis

Mice were randomly assigned to undergo CLP or sham surgery (n=10). One hour later, mice were treated with ibrutinib (30 mg/kg i.v.), acalabrutinib (3 mg/kg i.v.), or vehicle (5% DMSO + 30% cyclodextrin i.v.). Cardiac function was assessed 24 h after CLP surgery (n = 10 per group). **(A)** Illustration of the timelines of the CLP model. **(B)** Representative M-mode

echocardiograms. **(C)** Ejection fraction (%). **(D)** Fractional shortening (%). **(E)** Fractional area change (%). **(F)** CXCL10 serum concentration (pg/ml). **(G)** CXCL11 serum concentration (pg/ml). **(H)** correlation of ejection fraction and CXCL10 serum concentration. **(I)** Correlation of ejection fraction and CXCL11 serum concentration. All data are expressed as mean ± SEM for *n* number of observations. A value of ****$P < 0.0001$, ***$P < 0.001$, **$P < 0.01$, *$P < 0.05$ was considered to be statistically significant when compared to the control by one-way ANOVA followed by a Bonferroni's *post hoc* test. Correlations coefficients were determined by Pearson's correlation with *P* values based on two-tailed tests.
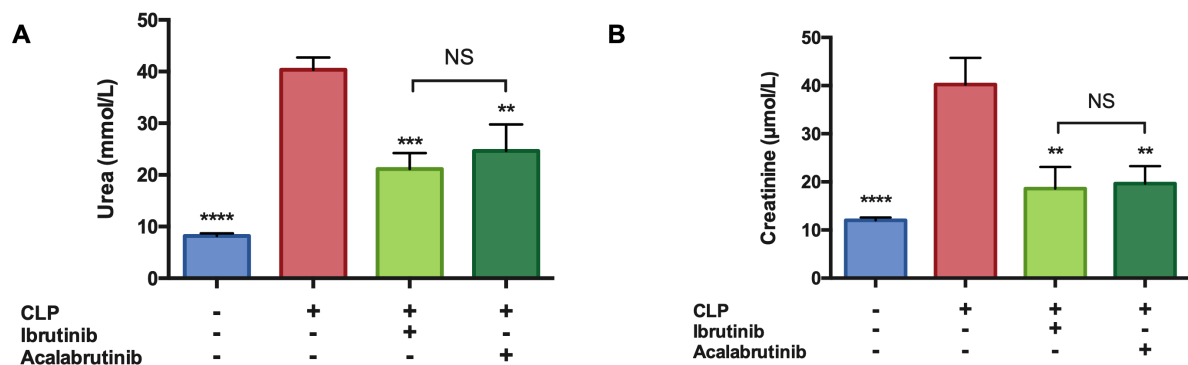
Figure 2: Ibrutinib or acalabrutinib attenuate the renal dysfunction caused by CLP-sepsis

Mice were randomly assigned to undergo CLP or sham surgery (n=10). One hour later, mice were treated with ibrutinib (30 mg/kg i.v.), acalabrutinib (3 mg/kg i.v.), or vehicle (5% DMSO + 30% cyclodextrin i.v.). At 24 h after CLP, blood samples were collected for analyses (n = 10 per group). **(A)** Serum urea (mmol/L). **(B)** Serum creatinine (µmol/L). All data are expressed as mean ± SEM for *n* number of observations. A value of ****$P < 0.0001$, ***$P < 0.001$, **$P < 0.01$, *$P < 0.05$ was considered to be statistically significant when compared to the control by one-way ANOVA followed by a Bonferroni's *post hoc* test.
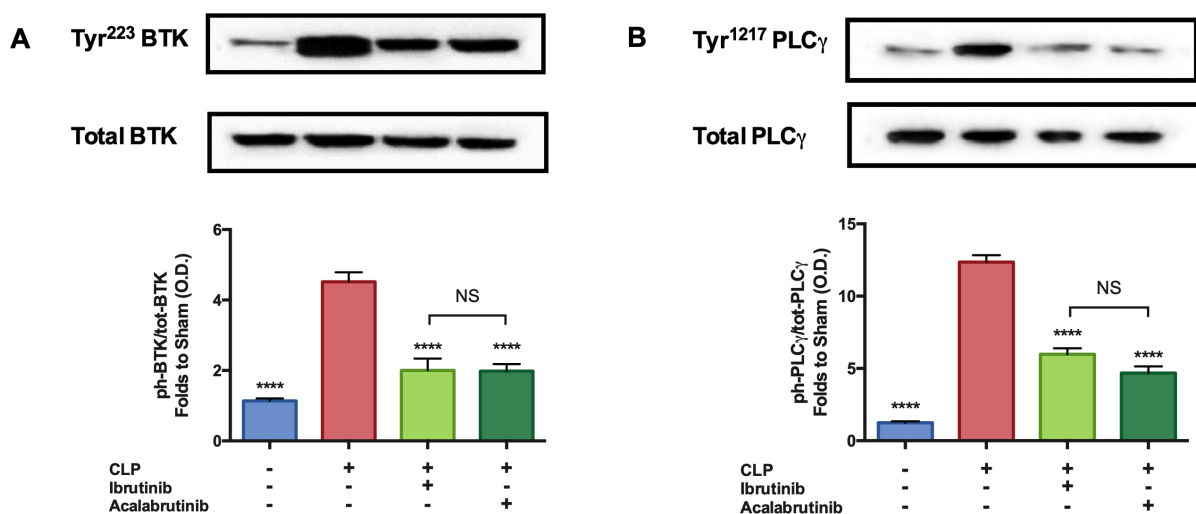
17

Figure 3: Cardiac BTK is activated in CLP mice and reduced by ibrutinib or acalabrutinib

Mice were randomly assigned to undergo CLP or sham surgery. One hour later, mice were treated with ibrutinib (30 mg/kg i.v.), acalabrutinib (3 mg/kg i.v.), or vehicle (5% DMSO + 30% cyclodextrin i.v.). At 24 h after CLP surgery, the activation of BTK in the heart was analyzed by western blot analysis (n=5 per group). Specifically, densitometric analysis of the bands is expressed as relative OD of **(A)** phosphorylation of BTK at Tyr^{223} corrected for the corresponding total BTK and normalized using the related sham band. **(B)** Phosphorylation of PLCγ at Tyr^{1217} corrected for the corresponding total PLCγ. All data are expressed as mean ± SEM for *n* number of observations. A value of ****$P < 0.0001$, ***$P < 0.001$, **$P < 0.01$, *$P < 0.05$ was considered to be statistically significant when compared to the control by one-way ANOVA followed by a Bonferroni's *post hoc* test.
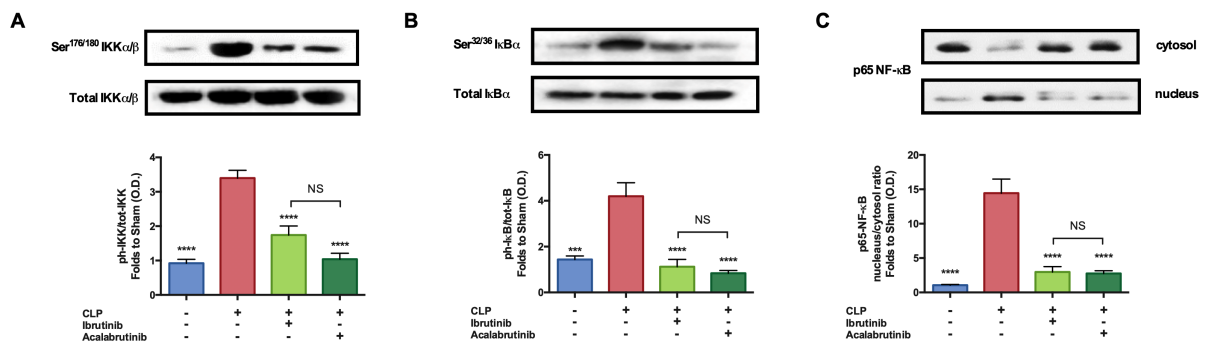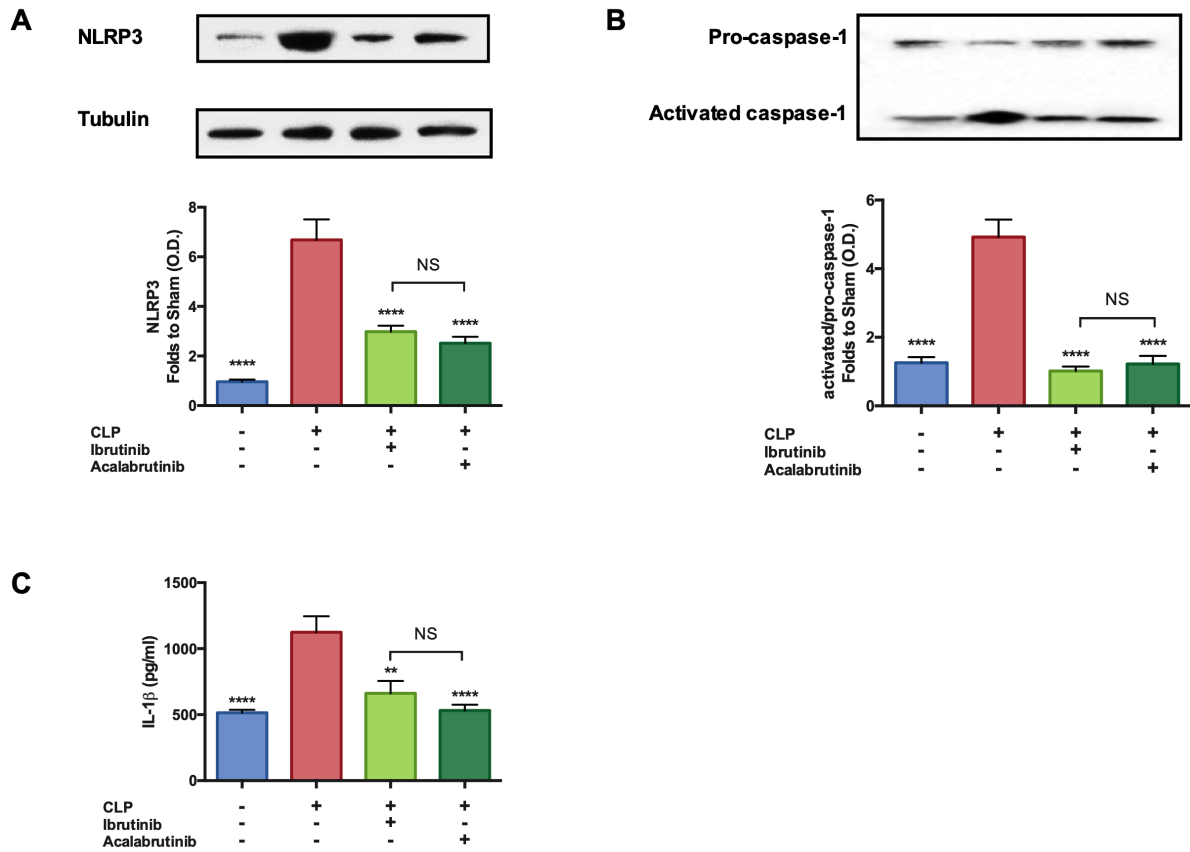

**Figure 4: Cardiac NF-κB activation in CLP mice is reduced by ibrutinib or acalabrutinib**

Mice were randomly assigned to undergo CLP or sham surgery. One hour later, mice were treated with ibrutinib (30 mg/kg i.v.), acalabrutinib (3 mg/kg i.v.), or vehicle (5% DMSO + 30% cyclodextrin i.v.). At 24 h cardiac tissue was collected and signaling was assessed (n = 10 per group). Densitometric analysis of the bands is expressed as relative OD of **(A)** phosphorylation of IKKα/β at $Ser^{176/180}$ corrected for the corresponding total IKKα/β and normalized using the related sham band. **(B)** Phosphorylation of IκBα at $Ser^{32/36}$ corrected for the corresponding total IκBα and normalized using the related sham band. **(C)** NF-κB p65 in both nucleus and cytosol and expressed as a ratio, normalized using the sham related bands. All data are expressed as mean ± SEM for *n* number of observations. A value of ****$P < 0.0001$, ***$P < 0.001$, **$P < 0.01$, *$P < 0.05$ was considered to be statistically significant when compared to the control by one-way ANOVA followed by a Bonferroni's *post hoc* test.

Figure 5: Cardiac NLRP3 activation in CLP mice is reduced by ibrutinib or acalabrutinib

Mice were randomly assigned to undergo CLP or sham surgery. One hour later, mice were treated with ibrutinib (30 mg/kg i.v.), acalabrutinib (3 mg/kg i.v.), or vehicle (5% DMSO + 30% cyclodextrin i.v.). At 24 h after CLP surgery, the assembly and activation of NLRP3 in the heart was analyzed by western blot analysis (n=5 per group). Specifically, densitometric analysis of the bands is expressed as relative OD of **(A)** NLRP3 activation, corrected against tubulin and normalized using the sham related bands. **(B)** Pro-caspase-1 against activated caspase-1 and normalized using the sham related bands. **(C)** IL-1β serum concentration analyzed by multiplex assay. All data are expressed as mean ± SEM for *n* number of observations. A value of ****$P < 0.0001$, ***$P < 0.001$, **$P < 0.01$, *$P < 0.05$ was considered to be statistically significant when compared to the control by one-way ANOVA followed by a Bonferroni's *post hoc* test.
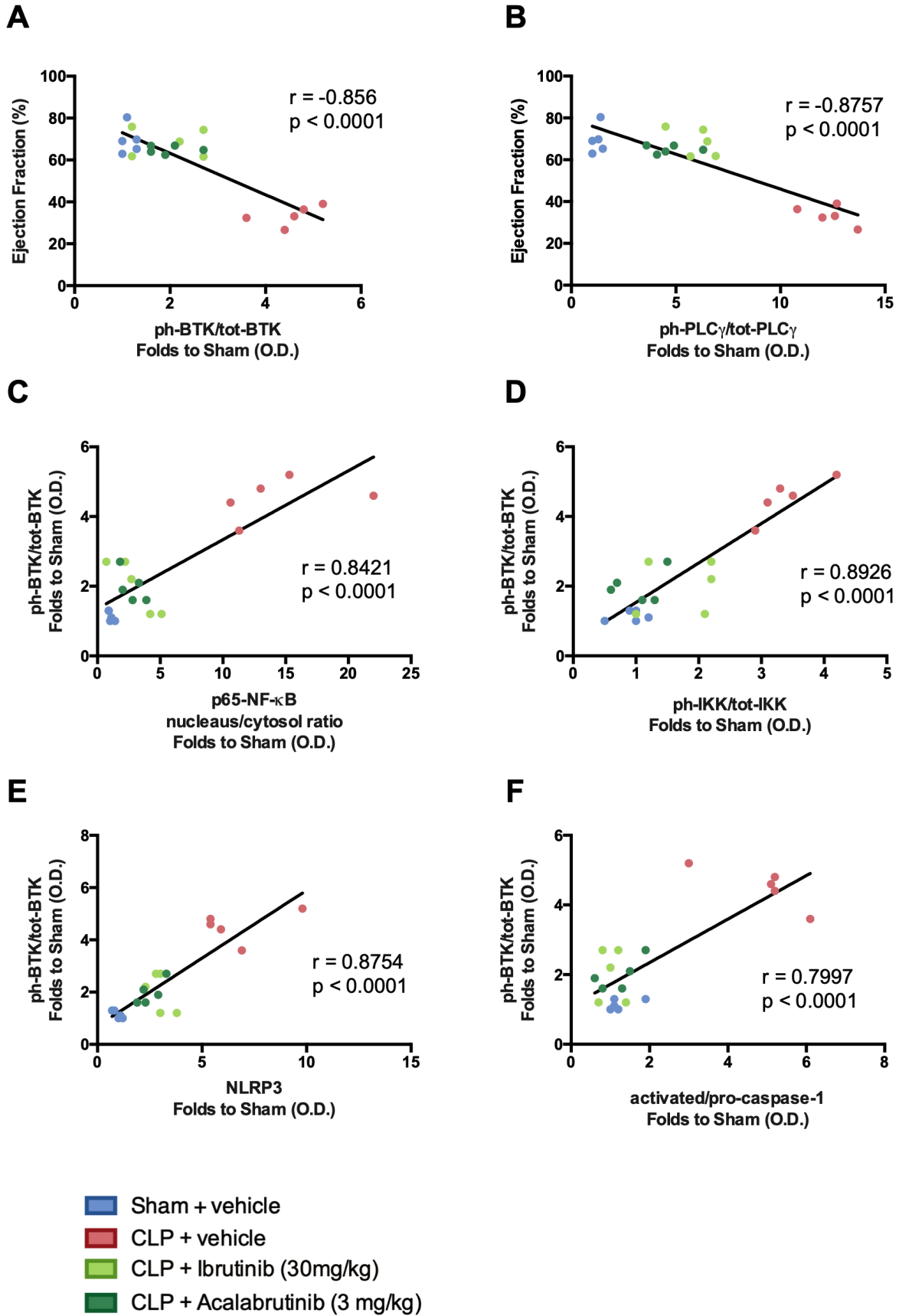
Figure 6: Relationship between BTK activation and cardiac dysfunction in CLP-sepsis

598 Correlation data to show **(A)** ejection fraction (%) vs. phosphorylation of BTK at Tyr^{223}. **(B)**
599 ejection fraction (%) vs. of PLCγ at Tyr^{1217}. **(C)** Phosphorylation of BTK at Tyr^{223} vs. NF-κB
600 p65. **(D)** Phosphorylation of BTK at Tyr^{223} vs. phosphorylation of IKKα/β at$\text{Ser}^{176/180}$. **(E)**
601 Phosphorylation of BTK at Tyr^{223} vs. NLRP3. **(F)** Phosphorylation of BTK at Tyr^{223} vs.
602 activated/pro-caspase-1. Data was analyzed by the Pearson correlation coefficient test to
603 calculate the r value and a two tailed T-test for significance, a value of ****$P < 0.0001$, ***P
604 < 0.001, **$P < 0.01$, *$P < 0.05$ was considered to be statistically significant.
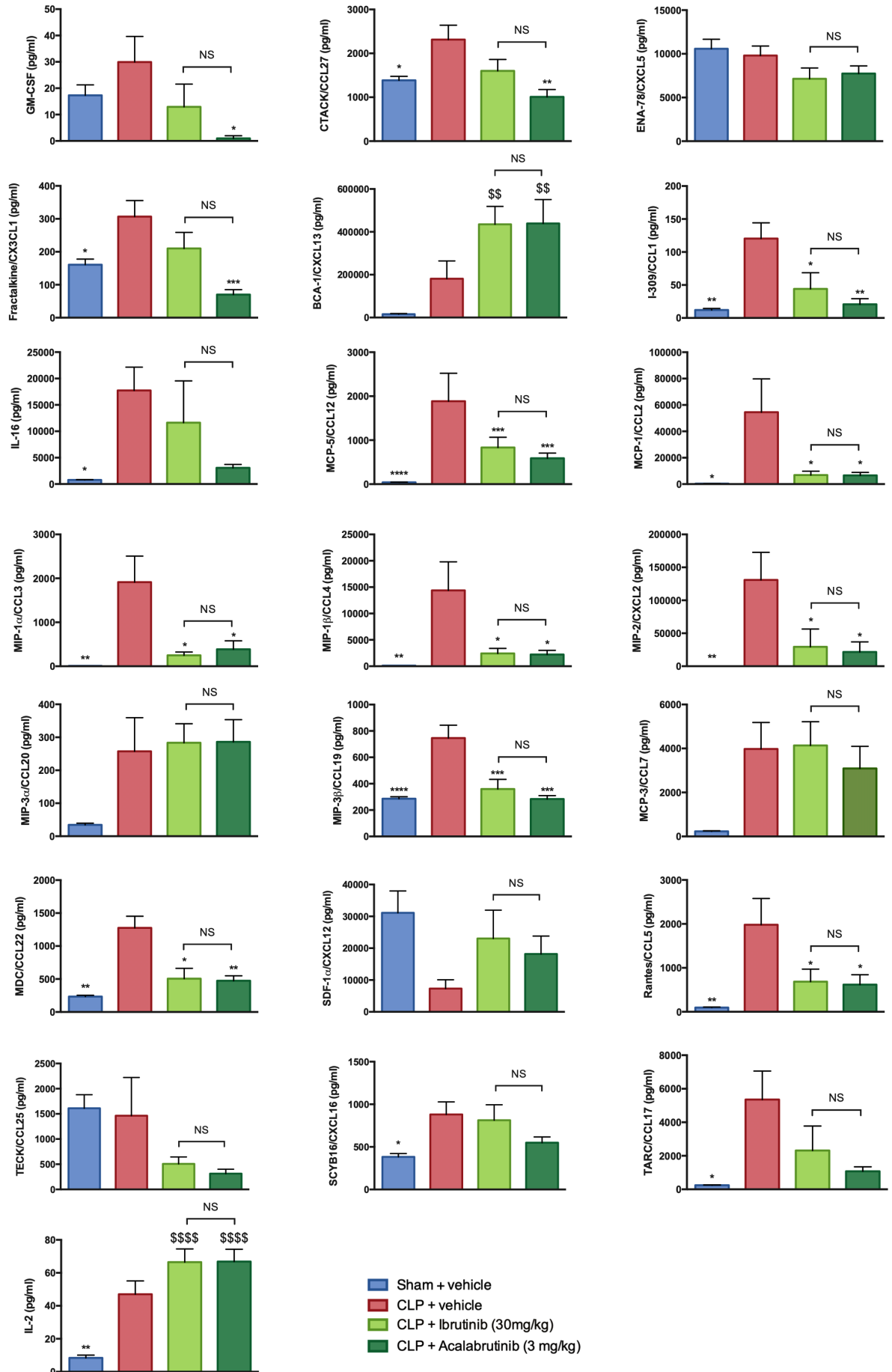
605
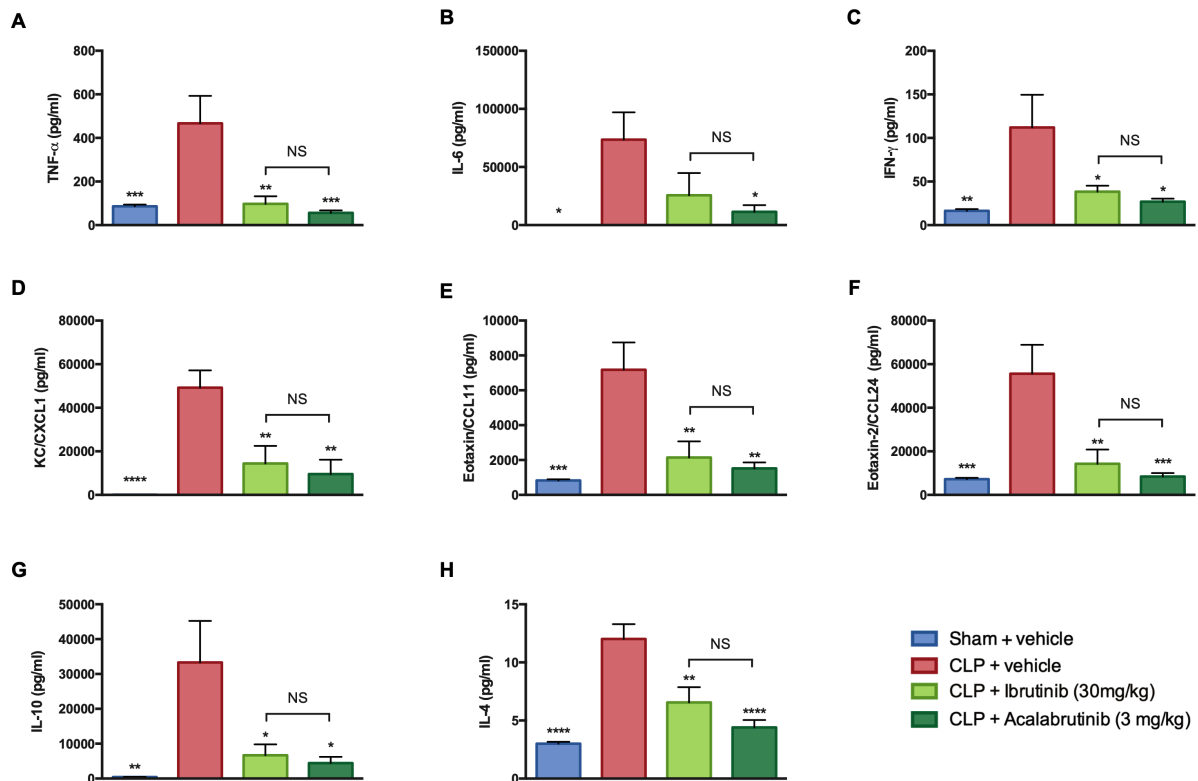
607 **Figure 7: Systemic inflammation in CLP mice is reduced by ibrutinib or acalabrutinib**

608 Mice were randomly assigned to undergo CLP or sham surgery. One hour later, mice were
609 treated with ibrutinib (30 mg/kg i.v.), acalabrutinib (3 mg/kg i.v.), or vehicle (5% DMSO +
610 30% cyclodextrin i.v.). At 24 h after CLP, blood samples were collected, and the serum
611 concentration of cytokines and chemokines were measured by a multiplex assay (n = 8 per
612 group). **(A)** TNF-α serum concentration (pg/ml). **(B)** IL-6 serum concentration (pg/ml). **(C)**
613 IFN-γ serum concentration (pg/ml). **(D)** KC/CXCL1 serum concentration (pg/ml). **(E)** Eotaxin-
614 1/CCL11 serum concentration (pg/ml). **(F)** Eotaxin-2/CCL24 serum concentration (pg/ml). **(G)**
615 IL-10 serum concentration (pg/ml). **(H)** IL-4 serum concentration (pg/ml). All data are
616 expressed as mean ± SEM for *n* number of observations. Correlations coefficients were
617 determined by Pearson's correlation with *P* values based on two-tailed tests a value of ****P
618 < 0.0001, ***$P < 0.001$, **$P < 0.01$, *$P < 0.05$ was considered to be statistically significant.

619

21

Supplementary figure 1: Systemic inflammation in CLP mice is reduced by ibrutinib or acalabrutinib

Mice were randomly assigned to undergo CLP or sham surgery. One hour later, mice were treated with ibrutinib (30 mg/kg i.v.), acalabrutinib (3 mg/kg i.v.), or vehicle (5% DMSO + 30% cyclodextrin i.v.). At 24 h after CLP, blood samples were collected, and the serum concentration of cytokines and chemokines were measured by a multiplex assay (n = 8 per group). All data are expressed as mean ± SEM for *n* number of observations. A value of ****$P < 0.0001$, *** $P < 0.001$, **$P < 0.01$, *$P < 0.05$ was considered to be statistically significant when compared to the control by one-way ANOVA followed by a Bonferroni's *post hoc* test. A value of $$$$$P < 0.0001$, $$$P < 0.01$, was considered to be statistically significant when compared to the sham by one-way ANOVA followed by a Bonferroni's *post hoc* test.